Journal of Environmental Sciences 167 (2026) 148–159

Contents lists available at ScienceDirect

Journal of Environmental Sciences

journal homepage: www.elsevier.com/locate/jes

JES JOURNAL OF ENVIRONMENTAL SCIENCES www.jesc.ac.cn

Research Article

Evidence of policy-driven emission reductions and post-pandemic rebound from high-resolution inventories in China

Wanyue Shan[a,b], Qing Wang[a,b], Ziang Ma[a,b], Xin Xu[a,b,*], Bofeng Cai[c,*], Xin Bo[a,b,*]

[a] Department of Environmental Science and Engineering, Beijing University of Chemical Technology, Beijing 100029, China
[b] BUCT Institute for Carbon-Neutrality of Chinese Industries, Beijing 100029, China
[c] Center of Carbon Neutrality, Chinese Academy for Environmental Planning, Beijing 100012, China

ARTICLE INFO

Keywords:
Air pollutants
Carbon dioxide
Integrative emission inventory
Reduction in pollution and carbon emissions
COVID-19 pandemic

ABSTRACT

Tracking emission changes throughout the Corona Virus Disease 2019 (COVID-19) pandemic is critical for revealing the impact of the pandemic on pollutant and carbon emissions; yet detailed assessments across this period remain limited. In this study, we developed integrative emission inventories for China in 2020 and 2023, and combined them with the inventory of 2018 to analyze national emissions of CO_2 and nine air pollutants before, during, and after the COVID-19 pandemic. Emissions were mainly concentrated in economically industrialized and developed provinces like Hebei, Shandong and Jiangsu, with higher emission intensities in energy-dependent provinces. 2020 saw notable declines in SO_2 (-18.1 %), VOCs (-32.6 %), and CO (-8.8 %) emissions compared to 2018 levels due to pandemic lockdowns and emission reduction policies, while CO_2 (11.6 %), NO_x (16.8 %), and PM_{10} (21.9 %) increased owing to expanded power generation and metal production. As economic activities rebounded in 2023, emissions of CO_2 (16.6 %) and nine air pollutants (3.2 %~15.1 %) increased compared with those in 2020, although adjustments in the energy structure helped reduce residential emissions of certain pollutants like PM and CO. Regionally, CO_2 emissions in the Beijing-Tianjin-Hebei (BTH), Yangtze River Delta (YRD), Pearl River Delta (PRD), and Fenwei Plain (FWP) regions continued to rise, while VOCs declined during the pandemic but rebounded afterward. The FWP region, dominated by heavy industry and fossil energy production, showed persistent $PM_{2.5}$ growth, facing greater challenges for emission reduction. These findings reveal the regional and sectoral emission dynamics throughout the COVID-19 pandemic, supporting integrated air pollutants and carbon management policies in China.

1. Introduction

Global climate change and air pollution have emerged as critical challenges to sustainable development. Greenhouse gas (GHG) and atmospheric pollutants emissions often originate from shared sources, and their intertwined effects exacerbate both air quality degradation and climate change, posing serious risks to environmental integrity and public health (Wang et al., 2023a; Wu et al., 2021b; Xu et al., 2022). Prolonged exposure to pollutants such as $PM_{2.5}$ and O_3 has been consistently linked to elevated risks of respiratory and cardiovascular diseases, contributing to increased rates of premature mortality (Liu et al., 2023). The persistent rise in carbon emissions driven by anthropogenic activities has intensified global warming and the frequency of extreme weather events, thereby further threatening human survival and socio-economic development. As the world's largest emitter of GHGs and atmospheric pollutants, China faces particular challenges in simultaneously mitigating climate change and air pollution, highlighting the need for integrated governance strategies.

In recent years, China has introduced a series of policies to promote coordinated management of carbon and air pollution (MEE, 2012; CPGPRC, 2013, 2018), supported by the development of national-scale emission inventories. Such comprehensive, data-driven approaches are indispensable for formulating effective climate and environmental policies, refining air quality governance, setting emission reduction benchmarks, and guiding energy policy. Key examples include the Multiresolution Emission Inventory for China (MEIC), providing a gridded dataset with a spatial resolution of 27 km × 27 km and covering CO_2 and nine air pollutants (SO_2, NO_x, CO, NMVOCs, NH_3, PM_{10}, $PM_{2.5}$, BC, and OC) from five major sectors (industry, power generation, transportation, resident, and agriculture) (Geng et al., 2024; Li et al., 2017). Based on extensive point-source data, Cai et al. (2018, 2019a, 2019b) constructed the China High-Resolution Emission Dataset (CHRED), which

* Corresponding authors.
E-mail addresses: 2023400082@buct.edu.cn (X. Xu), caibf@caep.org.cn (B. Cai), boxin@buct.edu.cn (X. Bo).

https://doi.org/10.1016/j.jes.2026.01.009
Received 30 June 2025; Received in revised form 6 January 2026; Accepted 6 January 2026
Available online 7 January 2026
1001-0742/© 2026 The Research Center for Eco-Environmental Sciences, Chinese Academy of Sciences. Published by Elsevier B.V.

provides multiyear, high-precision (1 km × 1 km) carbon emission inventories. Gao et al. (2022) further integrated CHRED with continuous emission monitoring system (CEMS) data, environmental statistics, emission permit reports, and data from the National Bureau of Statistics to develop CHRED 3.0A, an emission inventory for CO_2 and nine air pollutants in China for 2018, revealing the spatial (10 km × 10 km resolution) and temporal characteristics of these emissions. Similarly, Zhi et al. (2024) developed a national-scale inventory for 2019 that includes CO_2 and nine air pollutants, utilizing emission permit data and macroeconomic statistics at a spatial resolution of 0.1° × 0.1°, and examined the influence of economic development on emission patterns. Li et al. (2023) constructed the Air Benefit and Cost and Attainment Assessment System-Emission Inventory (ABaCAS-EI) v2.0, covering CO_2 and nine air pollutants from 11 emission sources across China (2005~2021) for long-term emission trend evaluation, with a spatial resolution of 27 km × 27 km. Despite these advancements, several critical limitations persist: (1) many national-scale inventories continue to rely on relatively coarse spatial resolutions, often at 27 km × 27 km, which limits their utility for fine-scale air quality and climate assessments; (2) while air pollutant inventories are increasingly integrated with carbon emission data, they typically account for NH_3 emissions from the agricultural sector but inadequately represent emissions from agricultural energy combustion such as the energy consumed in drying agricultural products (Li et al., 2023; Tong et al., 2020; Zhi et al., 2024); and (3) more notably, existing studies tend to focus on single-year estimates or short-term trends, lacking comprehensive evaluations of emission changes before, during, and after the Corona Virus Disease 2019 (COVID-19) pandemic. This limitation not only constrains a comprehensive understanding of the pandemic's disruptive effects and their long-term implications, but also underscores the need to investigate emission dynamics under major socio-economic perturbations.

The COVID-19 pandemic created an unprecedented disruption in economic and industrial activity. Strict containment measures led to marked declines in industrial output, transportation, and energy consumption, while stimulus policies initiated in May in 2020 and the full reopening of the economy by 2022 introduced new variations in emission trajectories (CPGPRC, 2020). Moreover, 2020 was a defining year for China's environmental and climate policy landscape. It marked the conclusion of the "13th Five-Year Plan" and the onset of preparations for the "14th Five-Year Plan," while also witnessing the formal announcement of China's dual-carbon strategy. This strategic shift signaled the beginning of a more structured and target-oriented approach to carbon mitigation. Understanding emission changes across pre-pandemic, pandemic, and post-pandemic periods is therefore essential to evaluate the combined effects of economic recovery and policy interventions.

To bridge these research gaps, this study utilizes multisource heterogeneous data, incorporating our team's power plant inventory (Qu et al., 2020; Tang et al., 2019), pesticide-use VOCs inventory (Chen et al., 2024) and independent coking industry inventory (Chen et al., 2023), to construct a national integrative emission inventory including CO_2 and air pollutants for 2020 (pandemic period) and update it to 2023 (post-pandemic period). The dataset covers the emissions of nine air pollutants and CO_2 from five sectors: power, industry, transportation, resident, and agriculture. Compared with our previously developed CHRED 3.0A inventory for 2018 (pre-pandemic period), we systematically analyze emission trends before, during, and after the COVID-19 pandemic. This study provides a refined and systematic characterization of China's current landscape of air pollutants and carbon emissions, offering robust data support and scientific evidence for formulating targeted strategies for coordinated pollution and carbon reduction, regional joint prevention and control, and sector-specific governance. More importantly, this study is the first to address the data gap on multisectoral emission changes following the opening of the pandemic in 2023. By capturing the evolving emission patterns before and after the pandemic, this work provides a solid foundation for understanding structural shifts and informing the design of a scientifically grounded pathway toward carbon peaking in the post-pandemic era.

2. Materials and methods

2.1. Source classification

For the national integrative emission inventory, emission sources were systematically categorized into five unified major sectors: power, industry, transportation, resident, and agriculture. Notably, the agricultural sector in this study encompassed not only ammonia emission sources but also the open burning of straw and the agricultural energy sub-sector. Agricultural energy mainly refers to the energy consumed for drying and heating in the agricultural, fishery, animal husbandry and forestry industries (excluding agricultural transportation and agricultural machinery that as non-road mobile sources in the transportation sector), such as the energy consumed in the initial processing of agricultural products, which contributes to both air pollutant and CO_2 emissions (MEE, 2024). A more detailed classification of sectoral emissions is presented in Appendix A Table S1, following the official guidelines (MEE, 2024).

2.2. Emission accounting

For emission accounting, emissions of air pollutants and CO_2 from the power sector, the independent coking industry, airports, and VOCs from pesticide use were derived from our team's previous research (Bo et al., 2021; Chen et al., 2024, 2023; Tang et al., 2019; Xu et al., 2024b; You et al., 2022). CO_2 emissions from all other sectors were sourced from CHRED (Cai et al., 2018, 2019a, 2019b) and were updated to 2020. CHRED is a high-accuracy and continuously updated carbon emission gridded dataset (10 km × 10 km) that has been widely applied in many studies (Cai et al., 2018, 2019a, 2019b; Gao et al., 2022; Jing et al., 2018; Liu et al., 2019; Wu et al., 2021a). Importantly, this study focused exclusively on direct CO_2 emissions (Scope 1) and did not account for indirect emissions. Building on this foundation, this study estimated air pollutant emissions from the remaining sectors via the emission factor method. Air pollutant and CO_2 emissions for each subsector were calculated on the basis of uniform activity level data, mainly from environmental statistics, emission permit reports, statistical yearbooks, industry reports and CHRED (Cai et al., 2018, 2019a, 2019b), as shown in Appendix A Table S1 in detail.

These datasets were reviewed based on the principles of normativity, completeness, consistency, and rationality. Taking the industrial sector as an example, China has established a multi-source environmental data management framework that includes environmental statistics, CEMS, and emission permit reports, which together contain extensive fundamental information. Data such as enterprise locations (with coordinates cross-verified using map applications) and equipment information were obtained from the environmental statistics database. Information on product types and outputs, raw and auxiliary material consumption, end-of-pipe treatment facilities, and stack parameters was extracted from the emission permit reports. For overlapping data among these databases, if discrepancies exceeded 60 %, further verification was conducted to ensure accuracy (Ran et al., 2019). For non-key industries, emission permits and statistical yearbooks were used as the primary sources of activity level data, supplemented by other relevant documentation like acceptance reports.

For the update of 2023 emission factors, this study comprehensively considered the recent progress in pollution control, the extent of ultra-low emission (ULE) standards, and changes in regulatory standards across industries to ensure that the estimates reflect the phased implementation of emission reduction policies. For the power sector, where ULE standards have been broadly implemented, emission factors were adjusted based on policy guidance (SCIOPRC, 2024), with eastern coal-fired units assumed to meet ULE standards and central-western

units assigned values close to more stringent limits to capture regional differences. For other industries, such as iron and steel, cement, and independent coking, emission factors were primarily updated using online monitoring data and publicly available information to reflect recent control improvements. Specifically, iron and steel factors were dynamically adjusted based on representative plant monitoring data; emission levels in the cement industry were calibrated using the annual average emissions of nationally monitored key enterprises, reflecting the progress of ultra-low emission retrofits since 2020; and coking emissions were adjusted minimally due to slower facility upgrades. All updated factors were normalized according to the statistical distribution of monitoring data and regulatory constraints to ensure methodological consistency and reproducibility.

The main formulas for calculating air pollutant emissions are as follows:

$$E = A \times \mathrm{EF}, \quad \text{without pollutant removal} \tag{1}$$

$$E = A \times \mathrm{EF} \times (1 - \eta), \quad \text{with pollutant removal} \tag{2}$$

where E (kg) represents pollutant emissions; A (t or 10^4 Nm^3) represents the activity level, such as fuel consumption or product output; EF (g/kg or kg/10^4 Nm^3) represents the pollutant emission factor; and η (%) represents the pollutant removal efficiency.

The main calculation formulas for CO_2 emissions are as follows:

$$E_{\mathrm{combustion}} = \sum_i \left(\mathrm{FC}_{i,j} \times \mathrm{NCV}_i \times \mathrm{CC}_i \times \mathrm{OF}_i \times 44/12\right) \tag{3}$$

$$E_{\mathrm{process}} = A \times \mathrm{EF}_{\mathrm{CO_2}} \tag{4}$$

where $E_{\mathrm{combustion}}$ (t) represents CO_2 emissions; E_{process} (t) represents CO_2 emissions; $\mathrm{FC}_{i,j}$ (t or 10^4 Nm^3) represents the consumption of fuel i required for the production of product j; NCV_i (GJ/t or GJ/10^4 Nm^3) represents the average low calorific value of fuel i; CC_i (t C/GJ) represents the carbon content per unit calorific value of fuel i; OF_i (%) represents the carbon oxidation rate of fuel i; 44/12 represents the molecular weight ratio of CO_2 to C; A (t) represents the output of product emitting CO_2 during the production process (Cai et al., 2018; Zhang et al., 2024); and $\mathrm{EF}_{\mathrm{CO_2}}$ (t CO_2/t product) represents the emission factor of CO_2.

2.2.1. Power

For the power sector, emissions of SO_2, NO_x, PM_{10}, and $PM_{2.5}$ were estimated at the facility level using a combination of CEMS-based emission factors and unit-specific fuel consumption data. The CEMS emission factors were derived from annual average pollutant concentrations and theoretical flue gas volumes for each power unit, thereby enhancing the accuracy and real-time applicability of the estimates, as outlined in Eq. (5). Emission calculations were conducted in accordance with Eq. (1) (Gao et al., 2022; Qu et al., 2020; Tang et al., 2019). For other pollutants, emission factors were selected from the *Technical Manual for the Compilation of City-level Air Pollutants Emission Inventory* (hereafter referred to as the *Technical Manual*), based on fuel type and combustion technology, with emissions computed using Eq. (2).

$$\mathrm{EF}_{f,u,s,p,h} = C_{f,u,s,p,h} \times V_{u,s,p,y} \tag{5}$$

where f, u, s, p, and h denote the pollutant species, facility, emission source, production process, and hour, respectively; y indicates the year; EF (g/kg) represents the emission factor for SO_2, NO_x, PM_{10}, and $PM_{2.5}$; C (g/m^3) is the pollutant concentration at the monitored emission outlet; and V (m^3/kg) denotes the theoretical flue gas volume.

CO_2 emissions were estimated primarily on the basis of the type and quantity of fuel consumed, as detailed in Eq. (3).

2.2.2. Industry

The industrial sector was classified into three primary subsectors: industrial energy use, industrial processes, and industrial solvent use.

For industrial energy, atmospheric pollutant emissions were estimated using Eq. (2), with emission factors sourced from the *Technical Manual*. Specifically, for coal combustion, emission factors for SO_2, PM_{10}, $PM_{2.5}$, BC, and OC were derived using material balance methods, in accordance with the *Technical Manual*.

For industrial processes, emissions of SO_2, NO_x, and PM from some priority controlled industries—such as cement, iron and steel, and independent coking—were estimated using CEMS-based emission factors (Bo et al., 2021; Tang et al., 2020, 2022), following the methodologies outlined in Eqs. (1) and (5). For other pollutants and industrial processes not covered by CEMS, emissions were calculated using Eq. (2), with emission factors also drawn from the *Technical Manual*.

Solvent use sources focused exclusively on estimating emissions of VOCs released during solvent application, as these activities do not emit CO_2. VOCs emissions were calculated via Eq. (2). For pesticide application, VOCs emissions were derived from the inventory developed in our previous research (Chen et al., 2024), whereas VOCs emission factors for other solvent-related industries were based on the literature listed in Appendix A Table S2.

CO_2 emissions were estimated based on the output of products emitting CO_2 during the production process, like cement clinker and electrolytic aluminum, as detailed in Eq. (4).

2.2.3. Resident

This sector encompassed emissions from civilian energy use—including the combustion of coal, oil, gas, and biomass—as well as emissions arising from household solvent use. It is important to note that biomass combustion for household purposes (excluding open burning) and residential solvent use are excluded from the CO_2 emission estimates. Carbon emissions were derived from the CHRED (Cai et al., 2018, 2019a, 2019b). Atmospheric pollutant emissions were estimated using an emission factor-based approach, with factors obtained from the *Technical Manual* and relevant literature cited in Appendix A Table S3. The calculation methodology followed the procedures specified in Eq. (1).

2.2.4. Transportation

Emissions from the transportation sector include both on-road and non-road sources, comprising tailpipe and evaporative emissions from road vehicles, as well as emissions from non-road mobile machinery and aviation. For on-road mobile sources, pollutant emissions were estimated using fuel consumption data from the CHRED, integrated with provincial-level data on vehicle types and fuel composition. Emission factors for air pollutants were sourced from the *EMEP/EEA Air Pollutant Emission Inventory Guidebook 2019* (EEA, 2019), with emissions calculated according to the methodology outlined in Eq. (1).

For evaporative emissions, according to the *EMEP/EEA Air Pollutant Emission Inventory Guidebook 2019*, the formula is as follows:

$$E_{\mathrm{VOCs}} = \sum_j \left(P_j \times EF_{\mathrm{VOCs},j} \times 365\right) \tag{6}$$

where E_{VOCs} (g/yr) represents the total evaporative VOCs emissions; P_j (vehicles) represents the number of gasoline vehicles of category j; and $EF_{\mathrm{VOCs},j}$ (g/(vehicle·day)) represents the VOCs emission factor for vehicle category j.

For non-road mobile sources, integrative emission inventories for civil aviation—covering both air pollutants and CO_2—were derived from previous research from our team (Xu et al., 2024a, 2024b; You et al., 2022). For other non-road sources, CO_2 emissions were obtained from the CHRED, whereas air pollutants were calculated via Eq. (1) on the basis of fuel consumption and the *Technical Manual*.

2.2.5. Agriculture

The agricultural sector inventory includes NH_3 emissions from livestock and poultry breeding, nitrogen-fixing crops, nitrogen fertilizer application, and human fecal matter, as well as air pollutant emissions from the open burning of straw and agricultural energy consumption.

Table 1 – Integrative emission inventory of nine air pollutants and CO_2 for China in 2020 (unit: Mt).

Sector	SO_2	NO_x	CO	$PM_{2.5}$	PM_{10}	BC × 100	OC × 100	VOCs	NH_3	CO_2
Power	0.56	1.16	6.83	0.08	0.10	0.03	0.08	0.26	0.00	5799.64
Industry	2.68	10.05	69.14	2.46	4.38	5.25	2.14	16.58	0.63	4731.26
Resident	2.05	0.38	24.10	1.57	1.77	30.31	74.68	1.58	0.13	520.43
Transportation	0.02	6.46	14.37	0.22	0.23	12.40	3.87	2.79	0.16	950.09
Agriculture	0.43	0.37	8.14	1.10	1.15	16.25	59.71	0.39	9.15	108.31
Total	5.75	18.42	122.59	5.43	7.63	64.24	140.48	21.59	10.05	12,109.73

For ammonia sources, emissions were estimated using activity data such as livestock and poultry population figures, nitrogen fertilizer application rates, the area cultivated with nitrogen-fixing crops, and the rural population lacking access to sanitary toilets. Calculations followed the methodology described in Eq. (1), with emission factors obtained from the *Technical Manual* and relevant literature (Fang et al., 2023; Gao et al., 2022).

For the open burning of crop residues, pollutant emissions were estimated from the amount of straw burned and emission factors provided in the *Technical Manual*. The amount of straw burned was calculated as follows:

$$A = P \times N \times R \times \eta \tag{7}$$

where A is the amount of straw burned, P is the crop yield, N is the grain-straw ratio, R is the open burning ratio, and η is the combustion efficiency. The parameter values were adopted from previous studies (Tian et al., 2011; Zhang, 2019).

Agricultural energy pertains to the consumption of energy for heating, drying, and various operations associated with agriculture, forestry, animal husbandry, and fisheries, excluding fuel usage by agricultural machinery and transportation vehicles. Emissions of air pollutants were estimated using methodologies consistent with those applied to residential energy consumption.

2.3. Spatial distributions

In this study, Geographic Information System (GIS) tools were utilized to spatially allocate emissions across 10 km × 10 km grid cells, facilitating the spatial characterization of emission sources. Point sources were assigned to their precise geographic locations whenever possible, based on the coordinates of individual enterprises. Location data for these enterprises were derived from environmental statistical records and other relevant datasets, and were further refined through visual interpretation from Google Earth, referencing imagery captured in the base year of the inventories. A manual calibration process was conducted to accurately identify the locations of emission outlets. Area sources were distributed spatially using the LandScan Global Population Dataset (Rose et al., 2021) (https://landscan.ornl.gov/) or the land use remote sensing monitoring dataset (https://www.resdc.cn/DOI/DOI.aspx?DOIID=54). Line sources, such as traffic-related emissions, were allocated according to the density of the road network within each grid cell. Further details regarding the spatial allocation methodology are presented in Appendix A Table S4.

3. Results and discussion

3.1. Sectoral emission analysis

3.1.1. Sectoral emissions in 2020

This section specifically analyzes the sectoral contribution of emissions, using 2020 as an example. The emissions of air pollutants and CO_2 from the five sectors of China in 2020 are shown in Table 1 (the sectoral emissions for China in 2023 are listed in Appendix A Table S5). For most air pollutants, industry was the main emitting sector, whereas power was the main sector for CO_2 emissions.

The contributions of each emission source to air pollutant and CO_2 emissions are shown in Figs. 1 and 2. CO_2 emissions were driven primarily by energy consumption, with the power sector—dominated by coal combustion—being the largest contributor (47.9 %), followed by industry (39.1 %). Supported by previous studies (Gao et al., 2022; Li et al., 2023; Zhi et al., 2024), the industrial and residential sectors were the primary contributors to SO_2, CO, PM_{10}, and $PM_{2.5}$ emissions. The major contributors to NO_x and VOCs were industry and transportation. In contrast, agriculture, which contributed negligible CO_2 emissions, was the predominant source of NH_3 emissions, accounting for over 91 %, primarily due to livestock farming and fertilizer application. Unlike previous studies, this research identified the agricultural sector, alongside the residential sector, as a major contributor to BC and OC emissions. This is largely attributable to the inclusion of both straw burning and agricultural energy combustion as agricultural emission sources in this study.

To further examine subsectoral contributions, Fig. 2 illustrates the breakdown within key emitting sectors. In the industrial sector, industrial boilers were the dominant source of CO_2, NO_x, and SO_2 emissions. Moreover, iron and steel production was the major contributor to CO emissions, whereas non-ferrous metal smelting significantly contributed to PM_{10} and $PM_{2.5}$ emissions. In the residential sector, coal combustion was the principal source of SO_2, CO, PM_{10}, and $PM_{2.5}$ emissions. In contrast, VOCs emissions were predominantly attributed to solvent use in industrial processes and on-road transportation. BC and OC emissions in the residential sector were primarily driven by coal and biomass combustion, whereas in the agricultural sector, straw burning emerged as the major contributor. These findings underscore the necessity for targeted mitigation strategies, with a particular emphasis on industrial boilers, solvent use, and residential coal combustion, to effectively reduce air pollution.

3.1.2. Sectoral emission changes during the COVID-19 pandemic

Fig. 3 shows the changes in the total emissions of nine atmospheric pollutants and CO_2 in China during the COVID-19 pandemic. Compared with the pre-pandemic emissions in 2018 (Gao et al., 2022), the total emissions of most pollutants declined in 2020. Notably, the emissions of VOCs decreased by 32.6 % (a reduction of 7040.5 kt), those of SO_2 decreased by 18.1 % (1042.1 kt), and those of CO decreased by 8.8 % (10.8 Mt). These reductions were primarily attributed to decreased industrial activity and traffic restrictions during the COVID-19 pandemic lockdown, along with the effective implementation of coal consumption reduction policies. In contrast, emissions of CO_2, NO_x, and PM_{10} in 2020 increased by 11.6 % (1402.3 Mt), 16.8 % (3091.8 kt), and 21.9 % (1674.3 kt), respectively, compared to 2018 levels. This increase was mainly due to the overall rise in thermal power generation and energy consumption in the power sector, driven by effective macroeconomic policies, despite the significant impact of lockdowns on the power and industrial sectors during the first quarter of 2020. Notably, while CO_2 emissions from the power sector increased, SO_2, $PM_{2.5}$, and PM_{10} emissions declined relative to 2018, reflecting the effectiveness of the ultra-low emission policy (Wu et al., 2022). Furthermore, adjustments in the energy structure of the industrial and residential sectors led to a marked increase in natural gas consumption, contributing to higher NO_x emissions. The rise in PM emissions was largely driven by increased production in the non-ferrous metal industry. Due to inconsistencies in the clas-

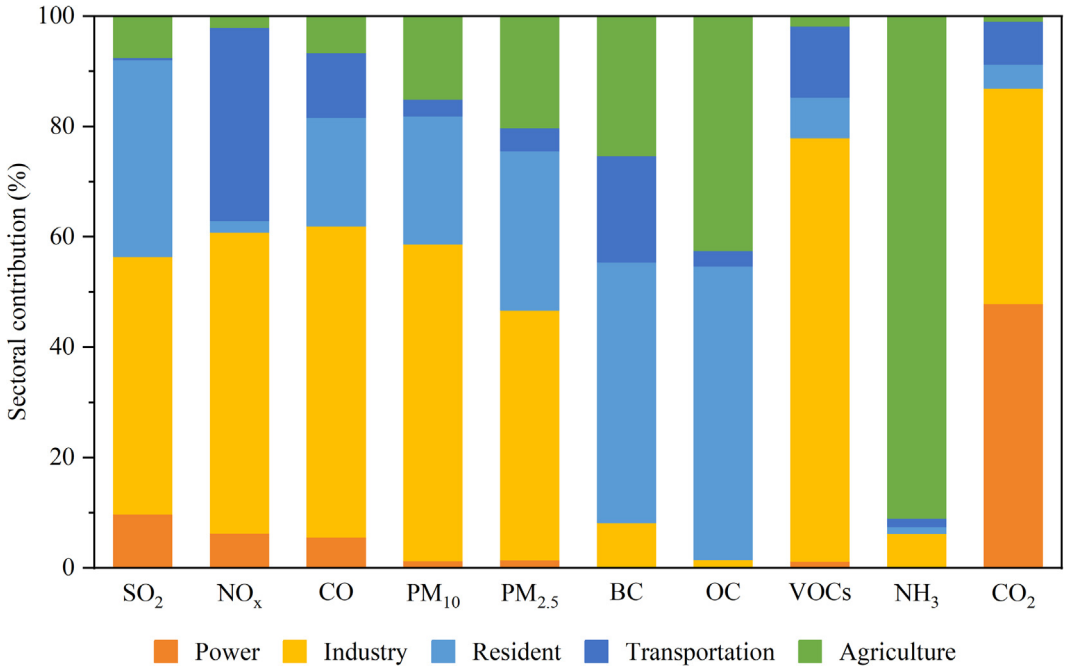


Fig. 1 – Sectoral emission contributions of CO_2 and air pollutants in 2020.

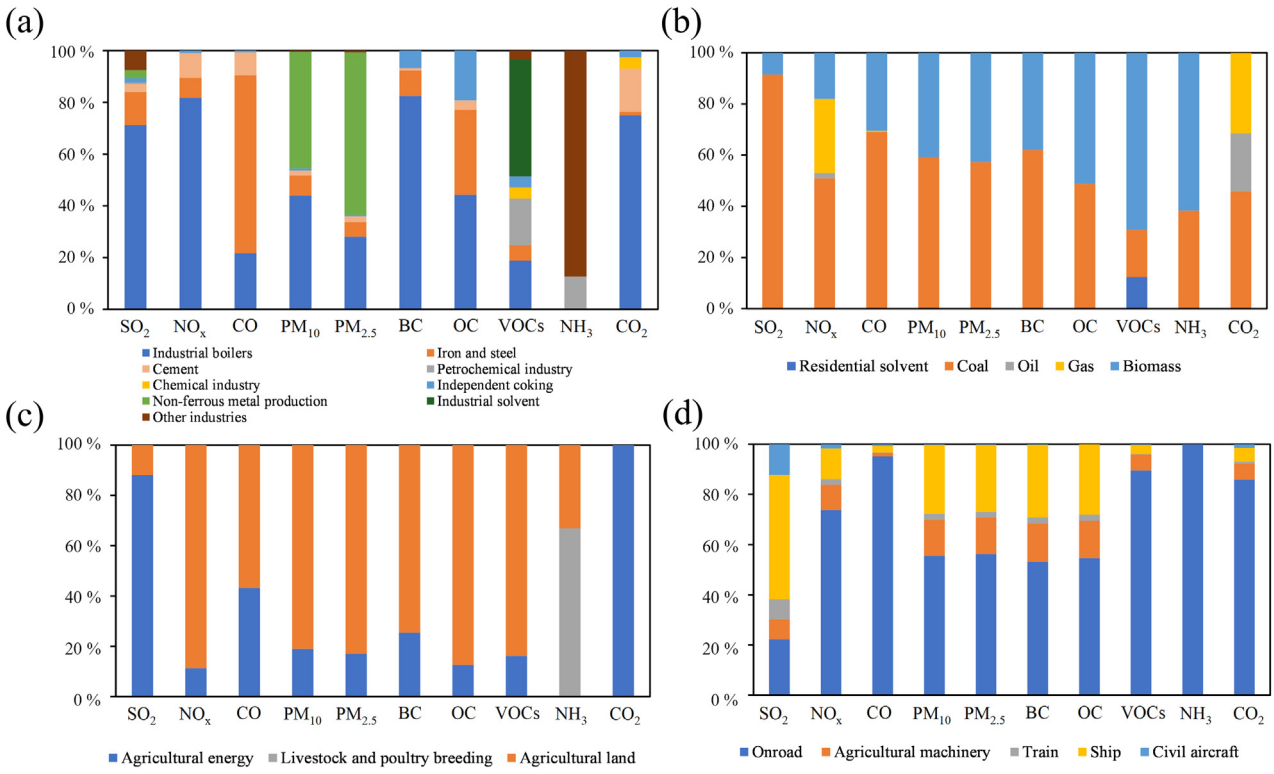


Fig. 2 – The fractional contributions of subcategories to CO_2 and air pollutants in China in 2020: (a) industry sector; (b) residential sector; (c) agriculture sector; (d) transportation sector.

sification of the residential and agricultural sectors between the 2018 and 2020 emission inventories, a sector-specific comparison was not conducted at this stage.

In 2023, following the relaxation of COVID-19 control measures and the continued resumption of economic activity, emissions of all major air pollutants and CO_2 increased relative to 2020 estimates. Compared with those in 2020, CO_2 emissions rose by 16.6 % (an additional 2083.9 Mt), with the majority of the increase originating from the industrial (1067.6 Mt) and power (779.3 Mt) sectors due to the growth in electricity and fossil energy demand. Achieving the dual-carbon goals remains a significant challenge. For air pollutants, SO_2 emissions increased by 185.7 kt (3.2 %), primarily driven by a 332.2 kt (12.4 %) rise in emissions from the industrial sector, offsetting notable declines in the residential (−110.5 kt) and agricultural (−71.8 kt) sectors due to structural adjust-

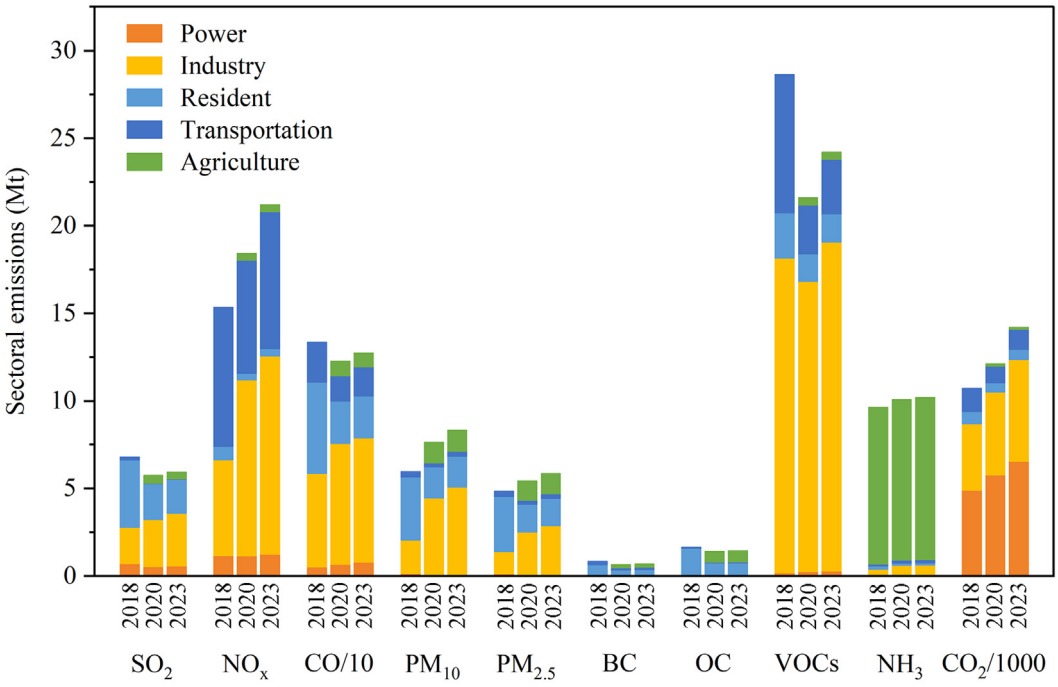


Fig. 3 – Changes in air pollutants and CO_2 emissions in China during the COVID-19 pandemic.

ments in energy consumption in these sectors. Emissions of NO_x (15.1 %, 2781.3 kt), CO (4.0 %, 4852.3 kt), VOCs (12.1 %, 2609.4 kt), PM_{10} (9.0 %, 683.7 kt), and $PM_{2.5}$ (7.8 %, 425.8 kt) increased driven mainly by the resurgence of industrial activities and increased traffic volume following the resumption of work and production. For example, the industrial sector increased the emissions of NO_x by 126.5 kt and VOCs by 219.3 kt, reflecting the intensification of manufacturing activities. Meanwhile, the transportation sector contributed 136.0 kt of increased NO_x and 34.0 kt of increased VOCs, indicating a rapid recovery in road transportation and logistics (Li et al., 2025; Wen et al., 2023). Nonetheless, compared to 2020, emissions of CO, PM_{10}, and $PM_{2.5}$ from the residential sector declined by 329.6, 11.6, and 5.8 kt, respectively. It was primarily resulted in the shifts in household energy structures, such as coal-to-gas and coal-to-electricity (Cao et al., 2025; Wang et al., 2023b; Wu et al., 2022; Xu et al., 2025). Emissions of NH_3, which were predominantly attributable to agricultural sources, increased slightly by 1.3 % (126.6 kt), indicating the relatively limited impact of the pandemic on agricultural emissions.

Excluding the anomalous effects of the COVID-19 pandemic in 2020, a comparison between 2023 and 2018 revealed that, despite increased activity levels across most sectors, emissions of SO_2, CO, BC, OC, and VOCs continued to decline by 856.4 kt, 6.0 Mt, 144.1 kt, 197.2 kt, and 4.3Mt, respectively. This trend underscores the effectiveness of emission reduction measures, especially residential energy structure adjustments and strengthened vehicle emission controls (Cao et al., 2025; Wang et al., 2023b; Wu et al., 2022; Xu et al., 2025). In contrast, emissions of PM_{10} and $PM_{2.5}$ increased by 2.4 Mt and 1.0 Mt, respectively, primarily due to the expansion of industrial activities, particularly in the non-ferrous metal sector, highlighting the need for more stringent air pollution control strategies targeting this industry.

This study systematically evaluated the impact of the COVID-19 pandemic on air pollutants and carbon emissions in China, elucidating the emission characteristics and underlying driving mechanisms during the lockdown measures implemented in 2020. This study revealed significant reductions in pollutants such as VOCs, SO_2, and CO in 2020 compared with those in 2018, which were driven primarily by decreased industrial activity, ultralow emission policies, and traffic restrictions. The study also captured, for the first time, the emission rebound associated with the full-scale economic recovery in 2023 following the lifting of pandemic control measures. Quantitative analysis demonstrated that the resurgence of industrial activities, increased traffic volumes, and rising energy consumption were key drivers of elevated emissions of NO_x, CO_2, SO_2, and VOCs, offering timely insights for ongoing policy refinement. Furthermore, the study examined the long-term effects of industrial and energy structure adjustments on emission trends, emphasizing the significant role of sustained reductions in coal consumption within the residential and agricultural sectors in mitigating PM and CO emissions. These findings highlight the potential of end-use energy structure optimization in achieving synergistic reductions in air pollutants and carbon emissions.

3.2. Spatial emissions analysis

3.2.1. Spatial emissions in 2020

The gridded (10 km × 10 km) spatial distribution of CO_2, NO_x, VOCs, and $PM_{2.5}$ across China in 2020 is presented in Fig. 4 (with other air pollutants shown in Appendix A Fig. S1). Most air pollutants exhibited spatial distribution patterns closely resembling that of CO_2, generally displaying greater concentrations in eastern regions compared to western areas. Emission hotspots were primarily located in central China (Henan), northern regions (Hebei, Shandong, Shanxi, Liaoning), and the southeastern coastal provinces (Jiangsu, Guangdong). These areas are marked by a high concentration of industrial enterprises—particularly energy-intensive industries—along with high population densities and dense road networks, resulting in substantial anthropogenic emissions of both air pollutants and carbon. This spatial pattern aligns with the findings of Zhi et al. (2024), further supporting the accuracy and reliability of the inventory developed in this study.

The provincial-level emissions of carbon and air pollutants in 2020 are presented in Appendix A Table S6, with sectoral proportion at the provincial level shown in Appendix A Fig. S2. Quantitatively, Shandong exhibited the highest CO_2 emissions (1042.29 Mt, accounting for 8.61 % of the national total), followed by Inner Mongolia (940.55 Mt, 7.77 %) and Jiangsu (915.73 Mt, 7.56 %). These provinces ranked among the top in terms of thermal power generation in China, and their CO_2 emissions were mainly contributed by the power sector (over 50 %). Hebei

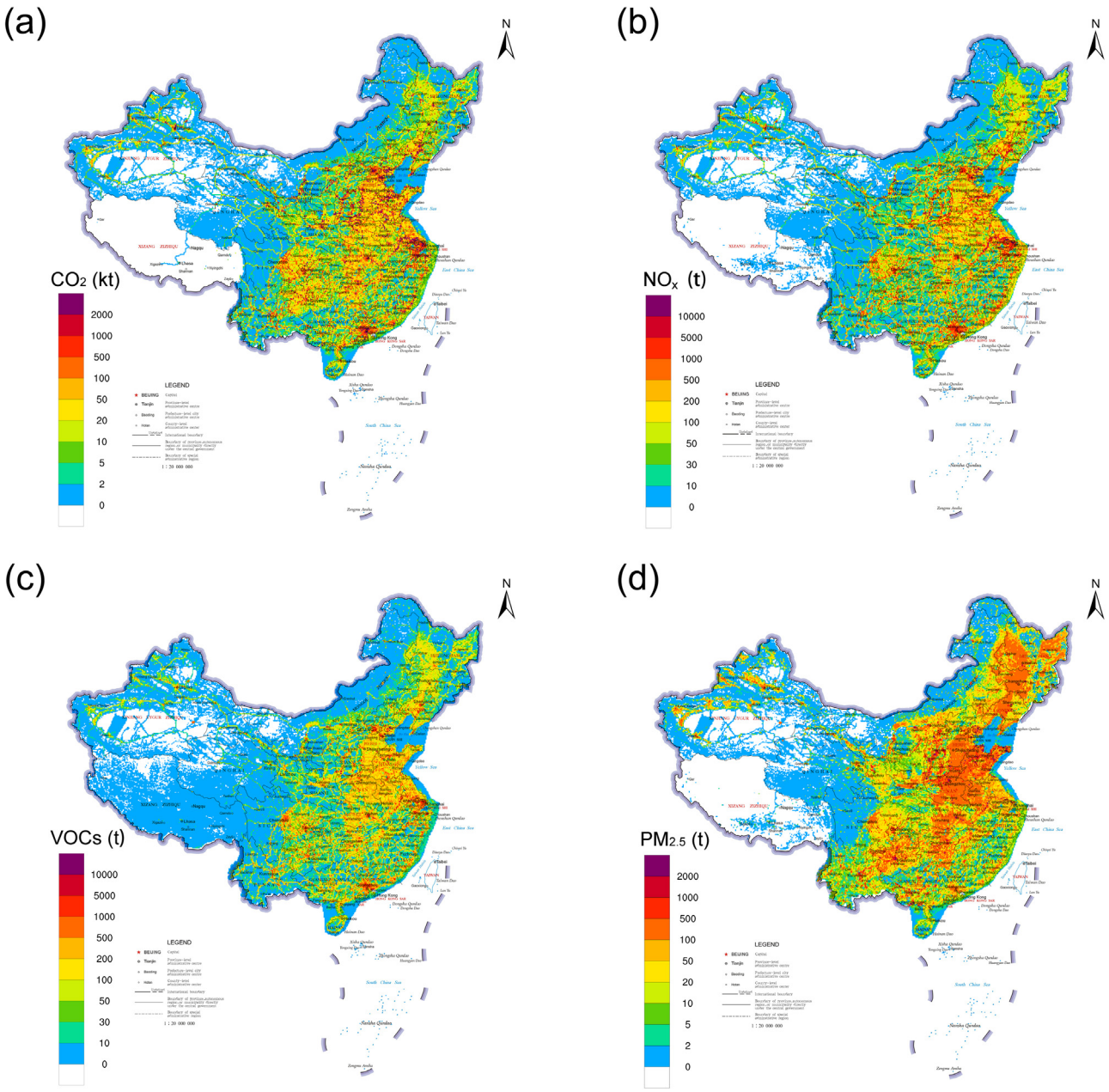


Fig. 4 – Gridded spatial distributions of CO_2 (a), NO_x (b), VOCs (c), and $PM_{2.5}$ (d) in China in 2020 (10 km × 10 km). The base map is from the Ministry of Natural Resources of the People's Republic of China (Review Number: GC(2019)1671).

recorded the highest SO_2 emissions (495.40 kt, accounting for 8.62 % of the national total), followed by Guizhou (454.41 kt, 7.91 %) and Shandong (437.26 kt, 7.61 %). In Hebei and Shandong, SO_2 emissions primarily originated from the industrial sector, contributing over 58 % of each province's total emissions, whereas in Guizhou, the majority of SO_2 emissions came from the residential sector, reflecting its coal-dominated energy structure. Hebei, Jiangsu, and Shandong ranked among the highest in emissions of NO_x, CO, and VOCs, where industry contributed >60 % even 80 % of local emissions, owing to their status as major energy consumers in the industrial sector and the presence of numerous high-emission enterprises, including those in the iron and steel, petrochemical, and chemical industries (Li et al., 2023). For PM_{10} and $PM_{2.5}$, the top three provinces were Shandong, Shanxi, and Henan, whose combined emissions accounted for over 30 % of the national total. This was mainly attributed to substantial industrial and residential coal consumption and the concentration of non-ferrous metal smelting industries, such as aluminum production (Zhi et al., 2024). Henan (800.37kt, accounting for 7.96 % of the national total), Shandong (700.27 kt, 6.96 %), and Inner Mongolia (638.69 kt, 6.35 %) also led in NH_3 emissions, largely attributed to their extensive livestock and poultry farming activities. Notably, pollutant and carbon emissions in Hubei Province remained comparatively low relative to other regions, a trend closely linked to the stringent lockdown measures enforced during the COVID-19 pandemic (Zheng et al., 2020).

To further understand urban emissions, Fig. 5 presents the prefectural-level emissions of CO_2 and some pollutants (NO_x, VOCs, and $PM_{2.5}$) in 2020 (other air pollutants shown in Appendix A Fig. S3). Cities with high emissions of many air pollutants are mainly industrially developed cities such as Tangshan, Chongqing, and Yuncheng, with VOCs being more concentrated in Hercynian, Chongqing, Yantai, Tangshan,

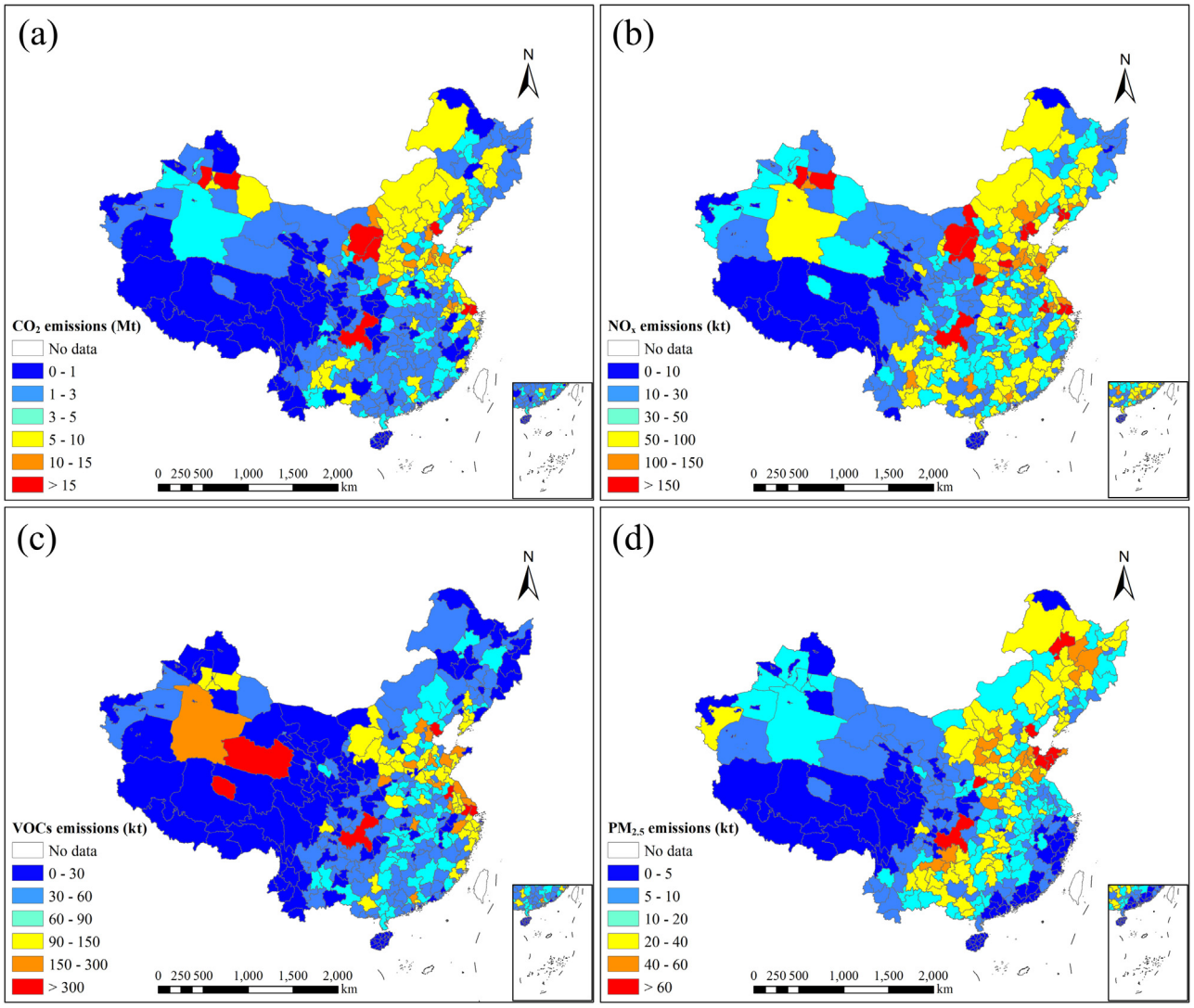


Fig. 5 – Prefectural-level spatial distributions of CO_2 (a), NO_x (b), VOCs (c), and $PM_{2.5}$ (d) in 2020.

Shanghai, and other petrochemical and chemical base cities. Cities with high CO_2 emissions are mainly concentrated in energy-intensive enterprises such as Tangshan, Ordos, Suzhou, Changji and Yulin.

3.2.2. Regional emissions changes during the COVID-19 pandemic

Across major regions of China, air pollutant emissions displayed distinct spatial and temporal variations before and after the COVID-19 pandemic (as shown in Fig. 6).

From 2018 to 2023, CO_2 emissions increased steadily in the BTH, YRD, and FWP regions, with average annual growth rates of 5.0 %, 4.7 %, and 7.7 %, respectively. In the BTH region, emissions increased steadily primarily driven by sustained energy demand from the industrial sector, as well as traffic volume and human activities after the release of the pandemic, despite efforts to promote electrification and coal substitution under the "14th Five-Year Plan" for ecological civilization construction (Li et al., 2025). The growth of the YRD region was mainly attributed to post-pandemic manufacturing rebounds and increased fossil fuel consumption in transportation, partially offset by regional energy structure adjustments. In the FWP region, due to its heavy reliance on coal-intensive industries like coking, where pollution control policies faced implementation challenges (Chen et al., 2023). Conversely, the PRD region saw a slight decline of 1.1 % during 2018~2020, largely resulting from reduced traffic volume and industrial activity during COVID-19 lockdowns, but emissions rebounded sharply by 25.4 % from 2020 to 2023, fueled by rapid economic recovery and heightened energy consumption in manufacturing (Zhang et al., 2026). Policy interventions (e.g., encouragement of electrification and coal substitution) have begun to reduce the carbon intensity in some sectors, but their impact on absolute CO_2 totals is still offset by growth in energy demand during the recovery period (NBSC, 2024a).

NO_x emissions in the BTH region increased by 83.8 % between 2018 and 2020, which was significantly higher than those in other regions. This spike was driven mainly by increased energy consumption in the architectural material and iron and steel industries, despite ongoing efforts to reduce capacity (NBSC, 2024b). The growth rate slowed to 12.2 % from 2020 to 2023 in the BTH region due to the recovery of economic activities and the increase in energy consumption for industry and transportation. In the YRD region, NO_x emissions increased with an average annual growth of 8.4 % largely contributed by industry in 2020 and transportation in 2023, whereas the emissions of the PRD and FWP regions kept steadily from 2018 to 2023.

VOCs emissions across the BTH, YRD, PRD, and FWP regions showed a consistent trend of decrease by 2020 followed by a rebound through 2023, with the emissions of the BTH and FWP regions maintaining stable levels overall. The 2020 decrease in the BTH, FWP, and PRD was mainly attributable to vehicle electrification and a sharp reduction in

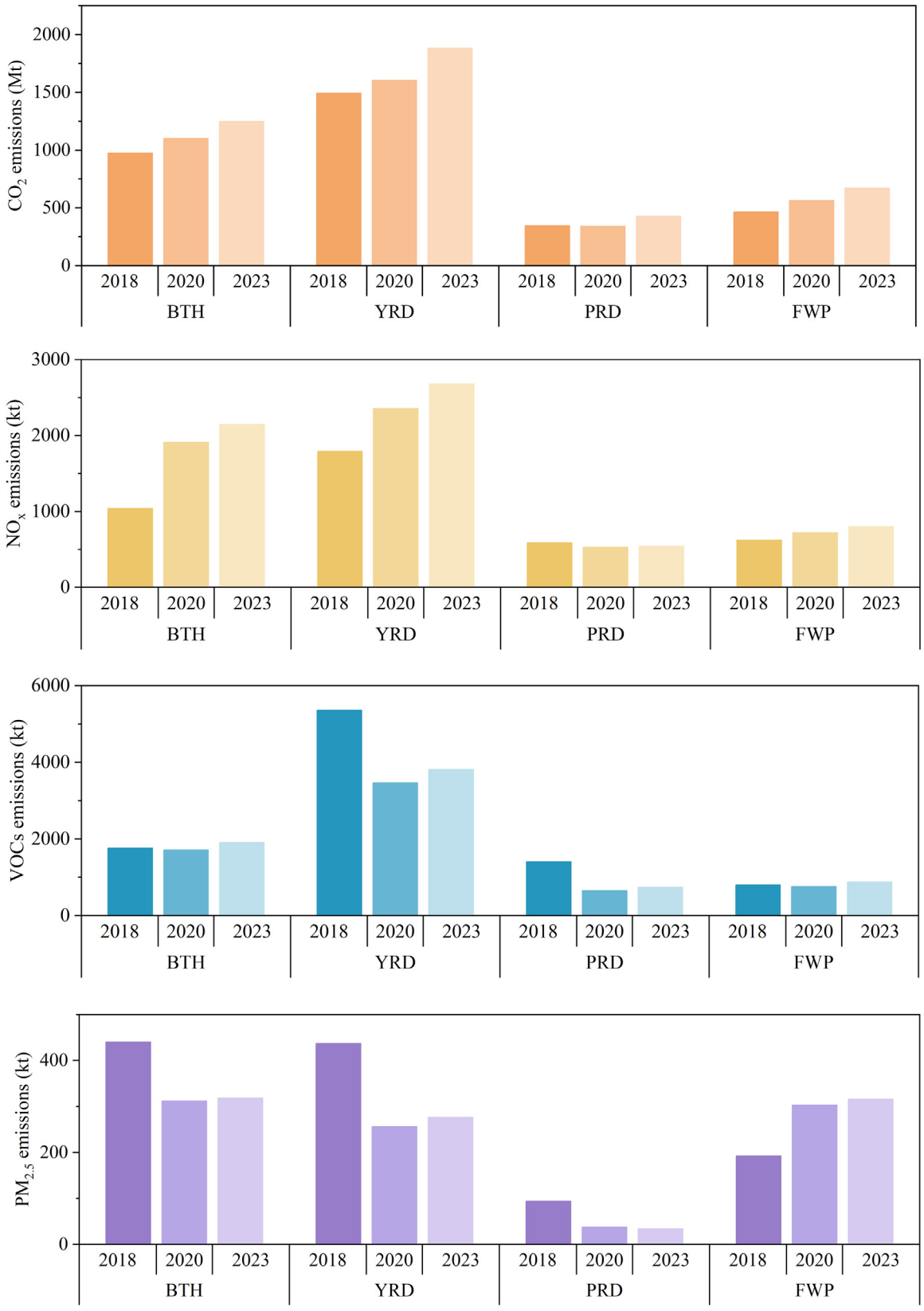


Fig. 6 – Changes in CO_2, NO_x, VOCs and $PM_{2.5}$ emissions in key regions during the COVID-19 pandemic. BTH: Beijing-Tianjin-Hebei; YRD: Yangtze River Delta; PRD: Pearl River Delta; FWP: Fenwei Plain.

Table 2 – Emissions of air pollutants and CO_2 per unit of GDP in China during the COVID-19 pandemic (unit: pollutant: kg/million yuan; CO_2: t/million yuan).

Year	SO_2	NO_x	CO	PM_{10}	$PM_{2.5}$	BC	OC	VOCs	NH_3	CO_2
2018	0.75	1.70	14.82	0.76	0.54	0.09	0.18	3.18	1.07	1.19
2020	0.57	1.81	12.07	0.75	0.53	0.06	0.14	2.12	0.99	1.19
2023	0.46	1.64	9.85	0.64	0.45	0.05	0.11	1.88	0.79	1.10

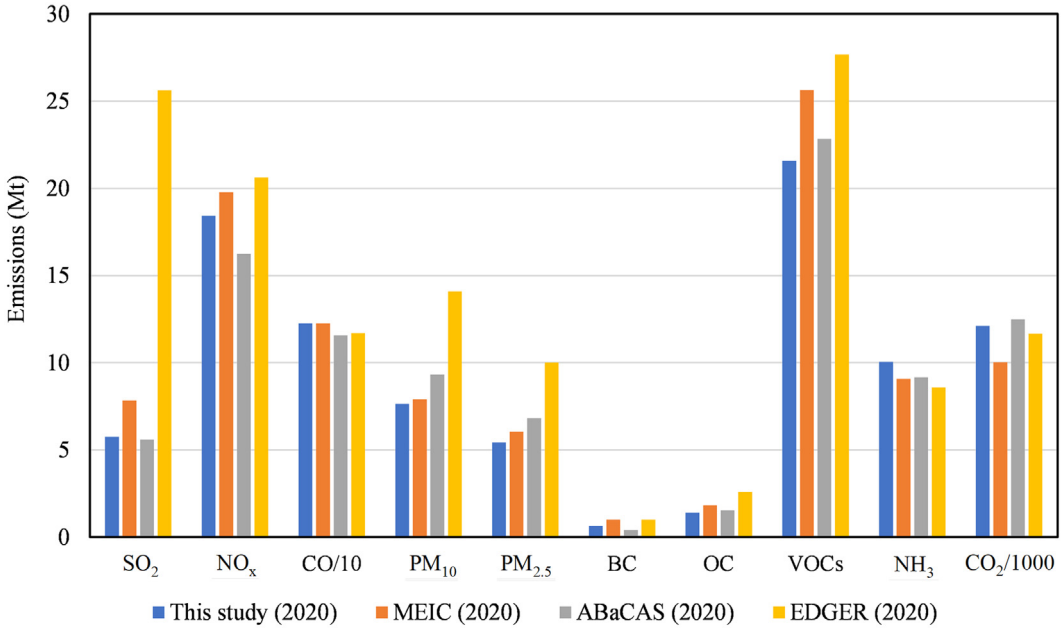


Fig. 7 – Comparison of this emission inventory with national emission inventories from other studies.

traffic volume during the COVID-19 pandemic, while the 2023 rebound was driven by increased industrial activity. In the YRD, the sharp decline of 53.6 % from 2018 to 2020 was primarily associated with the transportation sector, whereas the subsequent rise by 13.3 % in 2023 stemmed mainly from power generation activities.

Regarding $PM_{2.5}$ emissions, except for the FWP region, all these regions have achieved relatively good reduction results under the guidance of policies such as the *14th Five-Year Plan for Ecological Civilization Construction* and the *Action Plan for Winning the Blue Sky Defense Battle*, which emphasize active promotion of electrification and the reduction of coal consumption in residential and industrial uses. PRD emissions had the largest reduction and showed a continuous downward trend. The reduction rate reached 60.0 % from 2018 to 2020 and 10.4 % from 2020 to 2023, and mainly caused by the adjustment of industrial energy structure. In the YRD region, emission reduction mainly came from the ultra-low emission transformation of coal-fired power plants and the adjustment of regional energy structure (Yang, 2025). In contrast, the BTH region achieved a significant emissions reduction (29.2 %) in 2020 mainly through a substantial decline in residential coal consumption (Cao et al., 2025; He et al., 2025; Wang et al., 2023b). Although the FWP region has also actively implemented a variety of emission control measures—with notable improvements in the residential energy structure—the region remains one of China's key energy and chemical industry bases, hosting a dense concentration of coal, coking, iron and steel, power generation, and building material industries. Its heavy dependence on coal has led to a continued rise in PM emissions, highlighting the region's unique structural challenges and the greater complexity and difficulty of achieving deep emission reductions compared with other regions.

The temporal and spatial variations in emissions were driven by a complex interplay of socio-economic and policy factors. The YRD and BTH region demonstrated effective emission control in VOCs and $PM_{2.5}$ through advanced technology adoption, energy structure adjustment, ultra-low emission retrofits and pandemic lockdown of transportation, but rebounded in 2023. The PRD region sustained reductions via green industrial restructuring and stringent local regulations, such as the *Regulations on Air Pollution Prevention and Control of Guangdong Province*. In contrast, the BTH and FWP regions, reliant on traditional heavy industries faced rebounds due to slower industrial transformation, exacerbated by ongoing fossil fuel dependence. These trends underscore that the pandemic did not alter long-term emission trajectories. However, a green recovery pathway—prioritizing industrial restructuring, low-carbon technology deployment, stringent local regulations, and cross-regional coordination—is essential to achieve dual goals of air quality and climate mitigation.

3.3. Emissions per unit GDP across the COVID-19 pandemic

The provincial-level emissions per unit of GDP for carbon and air pollutants in 2020 are presented in Appendix A Table S7. The spatial distribution of emission intensity exhibited a consistent pattern across most pollutants, marked by pronounced spatial heterogeneity. Overall, provinces with high energy consumption—such as Shanxi, Inner Mongolia, Ningxia, and Xinjiang—recorded the highest emission intensities. In contrast, economically advanced regions like Beijing, Shanghai, and Guangdong, along with less industrialized provinces such as Tibet, displayed significantly lower emission intensities. At the national level, as shown in Table 2, emission intensities for all pollutants declined between 2018 and 2020, with the exception of NO_x increased by 6.5 % and CO_2 keep steadily.

3.4. Comparison and uncertainty analysis

This section compares the Chinese emission inventory developed in this study with the 2020 Chinese emission inventory datasets from MEIC (Geng et al., 2024), ABaCAS (Li et al., 2023), and EDGAR (Crippa et al.,

2024), as illustrated in Fig. 7. The overall emission ranges across these datasets are broadly consistent, with the notable exception of SO_2 emissions in the EDGAR dataset, which are significantly higher than those reported in the other three inventories. Compared to the results of this study, the MEIC and EDGAR datasets generally report higher emissions for most pollutants. This discrepancy is primarily attributed to the use of CEMS-based emission factors in this study for sectors such as thermal power, independent coking, iron and steel, and cement. These factors reflect the influence of ultra-low emission retrofits and are lower than guideline-based emission factors. Furthermore, the emission factors employed in this study are more temporally updated, enhancing their accuracy and relevance. In terms of the emissions of NH_3 and CO_2, this study is higher than those of the other inventories, mainly because this study also calculates ammonia emission sources such as nitrogen-fixing plants and human feces, which are not included in the calculations of the other datasets, and CO_2 accounts for a more detailed and comprehensive range of power plant emissions.

The emission inventories developed in this study are subject to certain uncertainties, primarily arising from the accuracy of activity level data and emission factors. Variations in data reporting scope, spatial resolution, and temporal coverage across different statistical sources introduce potential inconsistencies in activity levels for specific sectors and regions. Emission factors also exhibit variability due to differences in technology levels, fuel quality, and pollution control efficiencies. Although cross-validation among multiple databases reduced discrepancies, underestimation may still occur for small-scale industries and dispersed combustion sources. Overall, these uncertainties are not expected to alter the spatial distribution patterns or the dominant sectoral contributions but may introduce some uncertainties in the total emission estimates.

4. Conclusions and future prospects

By constructing high-resolution (10 km × 10 km) emission inventories for 2020 and 2023 and referencing a previously developed 2018 emission inventory, this study comprehensively evaluated the spatiotemporal evolution of air pollutant and CO_2 emissions across China at both national and regional scales during and after the COVID-19 pandemic. The results revealed significant emission declines in 2020 caused by pandemic lockdowns and emission reduction policies, followed by a rebound in 2023 driven by industrial and energy demand recovery. Distinct from previous research, this work was the first to integrate both air pollutants and carbon emissions from agricultural energy use into the agricultural sector inventory, enhancing the completeness of national emission accounting.

Specifically, in 2020, China's total emissions of SO_2, NO_x, CO, PM_{10}, $PM_{2.5}$, BC, OC, VOCs, NH_3, and CO_2 in China were 5.75, 18.43, 122.51, 7.64, 5.43, 0.64, 1.40, 21.63, 10.05, and 12786.41 Mt, respectively. CO_2 emissions were dominated by the power and industrial sectors; SO_2, CO, PM_{10}, and $PM_{2.5}$ by industrial and residential sources; NO_x and VOCs by industry and transportation; and NH_3 by agriculture. Spatially, emissions were concentrated in central, northern, and southeastern coastal provinces, while emission intensity was higher in energy-dependent regions such as Shanxi and Inner Mongolia. At the provincial level, Shandong, Inner Mongolia, and Jiangsu exhibited the highest CO_2 emissions, while Hebei ranked first in emissions of SO_2, NO_x, CO, and VOCs, PM_{10} and $PM_{2.5}$ were concentrated in Shandong, Shanxi, and Henan, and NH_3 in Henan, Shandong, and Inner Mongolia, reflecting regional variations in energy structure, industrial activity, and agricultural practices. Regionally, CO_2 emissions in BTH, YRD, PRD and FWP continued to increase, while VOCs generally declined during the pandemic but rebounded post-pandemic. Besides, the FWP region, as one of China's key heavy-industrial and fossil energy production bases, experienced a continuous rise in $PM_{2.5}$ emissions and is facing substantial pressure to achieve further emission reductions. These spatiotemporal emission patterns underscore the critical need for targeted policy and technological interventions to achieve coordinated reductions in both air pollutants and CO_2.

Achieving sustained co-reduction of air pollutants and carbon emissions requires long-term structural and technological measures. Priority actions include: (1) simultaneously accelerating the ultra-low emission transformation of heavy industrial boilers and process equipment; (2) promoting renewable energy deployment and improving energy efficiency are critical to decrease coal dependence and mitigate emissions from energy-intensive provinces such as Shanxi and Inner Mongolia; (3) strengthening cross-regional coordination and policy enforcement, particularly in the BTH and FWP regions, and addressing sector-specific drivers such as decarbonizing steel and transitioning coal to balance industrial growth with environmental and carbon goals; and (4) enhancing integrated data management and emission inventory systems to better quantify and monitor policy effectiveness. Future research should integrate high-resolution inventories with dynamic economic and energy models to capture feedbacks between policy actions, industrial activities, and emission trends. This study provides a robust data foundation and scientific guidance for post-pandemic environmental governance and high-quality development, supporting the synergistic advancement of air quality improvement and dual-carbon goals.

Data availability

The dataset applied for this study will be made available on request.

Declaration of competing interest

The authors declare that they have no known competing financial interests or personal relationships that could have appeared to influence the work reported in this paper.

CRediT authorship contribution statement

Wanyue Shan: Writing – original draft, Methodology, Formal analysis. **Qing Wang:** Software, Data curation. **Ziang Ma:** Software, Data curation. **Xin Xu:** Writing – review & editing, Validation, Supervision. **Bofeng Cai:** Supervision, Resources, Conceptualization. **Xin Bo:** Supervision, Resources, Funding acquisition, Conceptualization.

Acknowledgments

This work was supported by the Fundamental Research Funds for the Central Universities (No. buctrc202133) and the National Natural Science Foundation of China (No. 72174125).

Appendix A Supplementary data

Supplementary material associated with this article can be found in the online version at doi:10.1016/j.jes.2026.01.009.

References

Bo, X., Jia, M., Xue, X.D., Tang, L., Mi, Z.F., Wang, S.Y., et al., 2021. Effect of strengthened standards on Chinese ironmaking and steelmaking emissions. Nat. Sustain. 4 (9), 811–820.

Cai, B., Lu, J., Wang, J., Dong, H., Liu, X., Chen, Y., et al., 2019a. A benchmark city-level carbon dioxide emission inventory for China in 2005. Appl. Energy 233, 659–673.

Cai, B.F., Cui, C., Zhang, D., Cao, L.B., Wu, P.C., Pang, L.Y., et al., 2019b. China city-level greenhouse gas emissions inventory in 2015 and uncertainty analysis. Appl. Energy 253, 113579.

Cai, B.F., Liang, S., Zhou, J., Wang, J.N., Cao, L.B., Qu, S., et al., 2018. China high resolution emission database (CHRED) with point emission sources, gridded emission data, and supplementary socioeconomic data. Resour. Conserv. Recycl. 129, 232–239.

Cao, J., Liu, T.X., Ma, R., Sun, A., 2025. Antisocial responses to the "Coal to Gas" regulation: an unintended consequence of a residential energy policy. Manage. Sci. 71 (10), 8698–8726.

Chen, S.B., He, Y.J., Jiang, M.Y., You, Q., Ma, X.T., Xu, Z.J., et al., 2024. Unveiling the importance of VOCs from pesticides applicated in main crops for elevating ozone concentrations in China. J. Hazard. Mater. 465, 133385.

Chen, X.C., Li, J.H., Jia, M., Chen, S.B., Zhang, S.X., Bo, X., et al., 2023. High spatial resolution emission inventory of air pollutants and carbon in China's independent coking industry. Atmosphere 14 (2), 348.

CPGPRC (The Central People's Government of the People's Republic of China), 2013. Notice of The State Council on Printing and Distributing the Action Plan for the Prevention and Control of Air Pollution. Available at: https://www.gov.cn/zhengce/content/2013-09/13/content_4561.htm. Accessed 2013-09-13.

CPGPRC (The Central People's Government of the People's Republic of China), 2018. Notice of The State Council on Printing and Distributing the three-year action plan for winning the Blue sky defense battle. Available at: https://www.gov.cn/zhengce/zhengceku/2018-07/03/content_5303158.htm. Accessed 2018-07-03.

CPGPRC (The Central People's Government of the People's Republic of China), 2020. Solidly doing a good job in the "six stabilities", fully implementing the "six guarantees", and striving to complete the annual target tasks. Available at: https://www.gov.cn/xinwen/2020-05/25/content_5514580.htm. Accessed 2020-05-25.

Crippa, M., Guizzardi, D., Pagani, F., Schiavina, M., Melchiorri, M., Pisoni, E., et al., 2024. Insights into the spatial distribution of global, national, and subnational greenhouse gas emissions in the emissions database for global atmospheric research (EDGAR v8.0). Earth Syst. Sci. Data 16 (6), 2811–2830.

EEA (European Environment Agency), 2019. EMEP/EEA air pollutant emission inventory guidebook 2019. Available at: https://www.eea.europa.eu/en/analysis/publications/emep-eea-guidebook-2019. Accessed 2019-10-17.

Fang, L.J., Song, W.T., Yang, Y.Q., Qiong, Y.G., 2023. Inventory of anthropogenic ammonia emissions in Beijing-Tianjin-Hebei and its surrounding areas from 2008 to 2020. Res. Environ. Sci. 36, 500–509.

Gao, Y., Zhang, L., Huang, A.S., Kou, W.B., Bo, X., Cai, B.F., et al., 2022. Unveiling the spatial and sectoral characteristics of a high-resolution emission inventory of CO_2 and air pollutants in China. Sci. Total Env. 847, 157623.

Geng, G.N., Liu, Y.X., Liu, Y., Liu, S.G., Cheng, J., Yan, L., et al., 2024. Efficacy of China's clean air actions to tackle $PM_{2.5}$ pollution between 2013 and 2020. Nat. Geosci. 17 (10), 987–994.

He, Y.C., Wang, H.L., Zheng, Y.X., Feng, Y.Y., Chen, X.J., Jin, L., et al., 2025. Revealing air quality impacts of the clean heating campaign in northern China. Energy Econ. 141, 108078.

Jing, Q.N., Bai, H.T., Luo, W., Cai, B.F., Xu, H., 2018. A top-bottom method for city-scale energy-related CO_2 emissions estimation: a case study of 41 Chinese cities. J. Clean. Prod. 202, 444–455.

Li, M., Liu, H., Geng, G.N., Hong, C.P., Liu, F., Song, Y., et al., 2017. Anthropogenic emission inventories in China: a review. Natl. Sci. Rev. 4 (6), 834–866.

Li, S., Wang, S., Wu, Q., Zhang, Y., Ouyang, D., Zheng, H., et al., 2023. Emission trends of air pollutants and CO_2 in China from 2005 to 2021. Earth Syst. Sci. Data 15 (6), 2279–2294.

Li, Y.M., Zhang, Q.R., Liu, M.D., Yang, M.Q., Cai, X.R., Ye, J.S., et al., 2025. High spatiotemporal resolution inventory finely depicts the rebound characteristics of greenhouse gas emissions from vehicles in Beijing after the COVID-19 epidemic. Env. Sci. Technol. Lett. 12 (4), 405–412.

Liu, C., Chen, R., Sera, F., Vicedo-Cabrera, A.M., Guo, Y., Tong, S., et al., 2023. Interactive effects of ambient fine particulate matter and ozone on daily mortality in 372 cities: two stage time series analysis. Brit. Medi. J. 383, e075203.

Liu, H.L., Nie, J.X., Cai, B.F., Cao, L.B., Wu, P.C., Pang, L.Y., et al., 2019. CO_2 emissions patterns of 26 cities in the yangtze river delta in 2015: evidence and implications. Env. Pollut. 252, 1678–1686.

MEE (Ministry of Ecology and Environment of the People's Republic of China), 2012. Ambient air quality standards. China Environmental Science Press, Beijing.

MEE (Ministry of Ecology and Environment of the People's Republic of China), 2024. Notice on the issue of the "technical guidelines for the compilation of integrative emission inventories of air pollutants and greenhouse gases (trial)". Available at: https://wzq1.mee.gov.cn/xxgk2018/xxgk/xxgk06/202401/t20240130_1065242.html. Accessed 2024-01-30.

NBSC (National Bureau of Stastics of China), 2024a. China Energy Statistical Yearbook. https://data.cnki.net/yearBook/.

NBSC (National Bureau of Stastics of China), 2024b. China Statistical Yearbook. https://data.stats.gov.cn/easyquery.htm?cn=E0103.

Qu, J.B., Wang, P., Bo, X., Xue, X.D., Dong, G.X., Cui, L., et al., 2020. Inventory and distribution characteristics of China's thermal power emissions under ultra-low reconstruction. Environ. Sci. 41 (9), 7.

Ran, H.C., Lei, T.T., Bo, X., Tian, F., Qu, J.B., Ma, Y., et al., 2019. Research on the verification of industrial source emission inventory considering environmental management data: taking Cangzhou as an example. Env. Impact Assess. 41 (4), 46–49 +54.

Rose, A., McKee, J., Sims, K., Bright, E., Reith, A., Urban, M., 2021. LandScan Global 2020, 2020 Oak Ridge National Laboratory, Oak Ridge, TN.

SCIOPRC (The State Council Information Office of the People's Republic of China), 2024. China's energy transition. Available at: http://www.scio.gov.cn/zfbps/zfbps_2279/202408/t20240829_860395.html. Accessed 2024-08-29.

Tang, L., Jia, M., Bo, X., Xue, X.D., Guo, J., Tian, J., et al., 2020. High resolution emission inventory and atmospheric environmental impact research in Chinese iron and steel industry. China Env. Sci. 40 (4), 1493–1506.

Tang, L., Qu, J., Mi, Z., Bo, X., Chang, X., Anadon, L.D., et al., 2019. Substantial emission reductions from Chinese power plants after the introduction of ultra-low emissions standards. Nat. Energy 4 (11), 929–938.

Tang, L., Ruan, J.H., Bo, X., Mi, Z.F., Wang, S.Y., Dong, G.X., et al., 2022. Plant-level real-time monitoring data reveal substantial abatement potential of air pollution and CO_2 in China's cement sector. One Earth 5 (8), 892–906.

Tian, H.Z., Zhao, D., Wang, Y., 2011. Emission inventories of atmospheric pollutants discharged from biomass burning in China. Acta Sci. Circumstantiae 31 (2), 349–357.

Tong, D., Cheng, J., Liu, Y., Yu, S., Yan, L., Hong, C.P., et al., 2020. Dynamic projection of anthropogenic emissions in China: methodology and 2015–2050 emission pathways under a range of socio-economic, climate policy, and pollution control scenarios. Atmos. Chem. Phys. 20 (9), 5729–5757.

Wang, J., Lu, X., Du, P.F., Zheng, H.T., Dong, Z.X., Yin, Z.H., et al., 2023a. The increasing role of synergistic effects in carbon mitigation and air quality improvement, and its associated health benefits in China. Engineering 20, 103–111.

Wang, X., Sun, X., Ahmad, M., Zhang, H., 2023b. Does low carbon energy transition impede air pollution? Evidence from China's coal-to-gas policy. Resour. Policy 83, 103723.

Wen, Y.F., Liu, M., Zhang, S.J., Wu, X.M., Wu, Y., Hao, J.M., 2023. Updating on-road vehicle emissions for China: spatial patterns, temporal trends, and mitigation drivers. Env. Sci. Technol. 57 (38), 14299–14309.

Wu, N., Geng, G., Qin, X., Tong, D., Zheng, Y., Lei, Y., et al., 2022. Daily emission patterns of coal-fired power plants in China based on multisource data fusion. ACS Env. Au 2 (4), 363–372.

Wu, P., Guo, F., Cai, B., Wang, C., Lv, C., Liu, H., et al., 2021a. Co-benefits of peaking carbon dioxide emissions on air quality and health, a case of Guangzhou, China. J. Env. Manage. 282, 111796.

Wu, X., Li, D., Feng, M., Liu, H., Li, H., Yang, J., et al., 2021b. Effects of air pollutant emission on the prevalence of respiratory and circulatory system diseases in Linyi, China. Env. Geochem. Health 43 (11), 4475–4491.

Xu, X., Ma, Z., Zhang, Z., Qu, J., Bo, X., Zhang, Y., 2025. Substantial emission reductions from chinese iron- and steelmaking after the introduction of ultralow emission standards during the Prepandemic and Midpandemic periods. ACS ES&T Air 2 (11), 2550–2565.

Xu, X., Yang, H., Li, C., 2022. Theoretical model and actual characteristics of air pollution affecting health cost: a review. Int. J. Env. Res. Public Health 19 (6), 3532.

Xu, X., You, Q., Zhang, Z., Zhang, B.D., Bo, X., Wang, Z.T., 2024a. Air pollutants and carbon emission inventory of civil aviation airports in China in the scenario of peak carbon dioxide emissions. Acta Sci. Circumstantiae 44, 428–437.

Xu, X., You, Q., Zhang, Z., Zhao, Z.M., Wang, Z.T., Zhang, B.D., et al., 2024b. Insights into civil aviation emissions in China: analysis of an emission inventory of air pollutants and the ChinaHighAirPollutants (CHAP) dataset. Atmos. Env.: X 22, 100270.

Yang, Y., 2025. Study on the integrated emission inventory of air pollutants and greenhouse gases from china's thermal power industry and its environmental impact. Master thesis. Beijing University of Chemical Technology, Beijing, China.

You, Q., Li, H.M., Bo, X., Zheng, Y., Chen, S.B., 2022. Air pollution and CO_2 emission inventory of Chinese civil aviation airport. China Env. Sci. 42 (10), 4517–4524.

Zhang, L., Ruan, J.H., Zhang, Z., Qin, Z.Y., Lei, Z.Y., Cai, B.F., et al., 2024. City-level pathways to carbon peak and neutrality in China. Cell Rep. Sustain. 1 (5), 100102.

Zhang, L., Shan, W.Y., Meng, F.X., Zhu, S.Y., Niu, M.C., Du, M.B., et al., 2026. Note unexpected reverse in city-level CO_2 carbon peak status: challenges to China's ambitious climate goals. Env. Impact Assess. Rev. 117, 108176.

Zhang, X., 2019. Research On High-Resolution Emission Characteristics of Air Pollutants from Straw Burning in China. Master thesis. Nanjing University, Nanjing, Jiangsu, China.

Zheng, B., Geng, G.N., Ciais, P., Davis, S.J., Martin, R.V., Meng, J., et al., 2020. Satellite-based estimates of decline and rebound in China's CO_2 emissions during COVID-19 pandemic. Sci. Adv. 6 (49), eabd4998.

Zhi, G.R., Du, J.H., Chen, A.Z., Jin, W.J., Ying, N., Huang, Z.H., et al., 2024. Progression of an emission inventory of China integrating CO_2 with air pollutants: a chance to learn the influence of development on emissions. Atmos. Env. 316, 120184.